Prof. Y. W. Lee
Prof. A. G. Bose
Prof. A. H. Nuttall
D. A. Chesler
W. M. Cowan, Jr.
D. A. George
A. D. Hause
I. M. Jacobs
K. L. Jordan, Jr.
M. Schetzen
D. W. Tufts
C. E. Wernlein (Absent)
G. D. Zames

A. MEASUREMENT OF FIRST- AND SECOND-ORDER PROBABILITY DENSITIES

Recently, a digital probability density analyzer was constructed for operation in conjunction with the M.I.T. digital correlator (1). The description and construction details of the analyzer are given elsewhere (2, 3) together with a few experimental results. Some more experimental results are given here; in particular, a measurement of the second-order probability density of a random process generated by passing the noise output of a gas triode through a narrow-band filter.

The measured first-order probability density for a triangular wave is shown in Fig. XI-1, and for the noise output of a 6D4 gas triode in Fig. XI-2. The use of a 6D4 gas triode as a noise generator has been described by Cobine (4) and he noted that the output has a probability density that is not quite Gaussian, as can be seen from Fig. XI-2. The effect is more noticeable on an oscilloscope on which the noise appears slightly asymmetric for the extreme peaks. The noise may be made more nearly Gaussian by passing it through a narrow-band filter. Figure XI-3 shows the probability density of the noise, after it has been passed through a filter of center frequency 80 kc and bandwidth 5 kc.

In Fig. XI-3 a comparison is made between the recorded experimental points and a curve labeled "theoretical." This curve is not theoretical in the usual sense of the word, since the mean and variance of the curve are not known a priori. The system of measurement introduces a gain and a dc level, neither of which can be ascertained exactly. The theoretical curve is then a best-fit curve. The ideal method for finding the best-fit curve would be to define a measure D of the deviation (say, mean-square error) of the experimental points from a theoretical curve and choose that Gaussian curve with such mean and variance that D is minimized. Then a test of "goodness-of-fit" (5) could be applied for justification of the hypothesis that the process has a first-order Gaussian probability density. A graphical method that utilizes the same principle was employed here. It consists of assuming a mean (an accurate guess would be the mean for the measured distribution) and plotting the logarithm of the probability density against the square of the deviation from the mean. A true Gaussian curve with such a mean would be a straight line with slope

$$s = -\frac{\log_{10} e}{2\sigma^2}$$

as can be seen by taking the Gaussian density

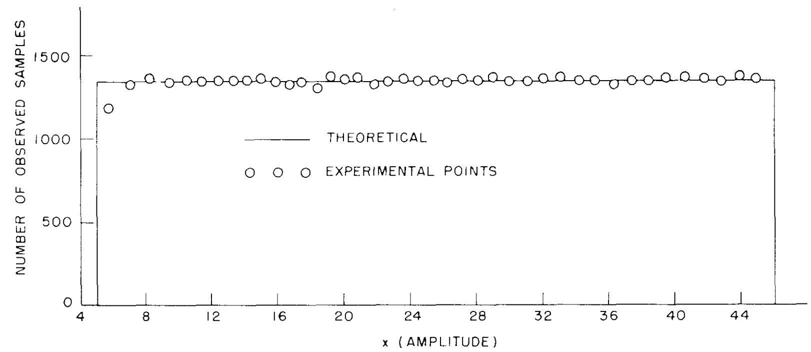

Fig. XI-1. Probability density of triangular wave.

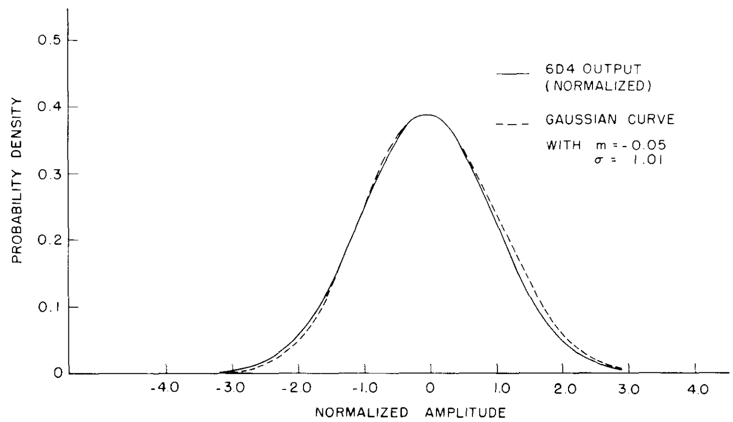

Fig. XI-2. Probability density of Sylvania 6D4 gas triode output.

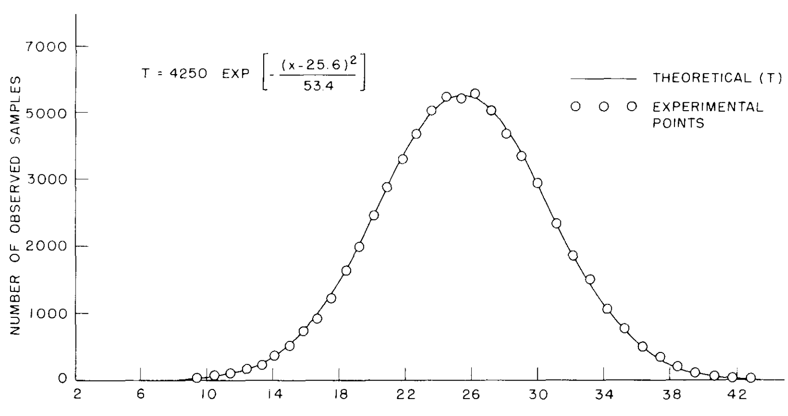

Fig. XI-3. First-order probability density of Gaussian noise.

$$p(x) = \frac{1}{\sqrt{2\pi}\,\sigma} \exp\left[-\frac{x^2}{2\sigma^2}\right]$$

and taking the logarithm of both sides. Then

$$\log_{10} p(x) = \log_{10} \frac{1}{\sqrt{2\pi}\,\sigma} - \frac{\log_{10} e}{2\sigma^2} x^2$$

If the wrong mean has been chosen, the line for $x > 0$ will be slightly displaced from the line for $x < 0$. A straight line is then drawn through the points for a best fit.

In Fig. XI-4 a plot of the experimental points of a second-order probability density of two samples of the noise 4 μsec apart is shown. It is slightly more complicated to find a best-fit curve for such a density. As seen from the joint probability density of two random variables (6),

$$p(x_1, x_2) = \frac{1}{2\pi\,\sigma_1\sigma_2(1-\rho^2)^{1/2}} \exp\left[-\frac{\sigma_2^2(x_1-m_1)^2 - 2\sigma_1\sigma_2\rho(x_1-m_1)(x_2-m_2) + \sigma_1^2(x_2-m_2)^2}{2\sigma_1^2\sigma_2^2(1-\rho^2)}\right] \tag{1}$$

there are five parameters, which are the variances, σ_1 and σ_2; the means, m_1 and m_2; and the correlation coefficient, ρ. The parameters σ_1, m_1 are not necessarily equal to σ_2, m_2 because the two samples are sent through independent channels in the correlator.

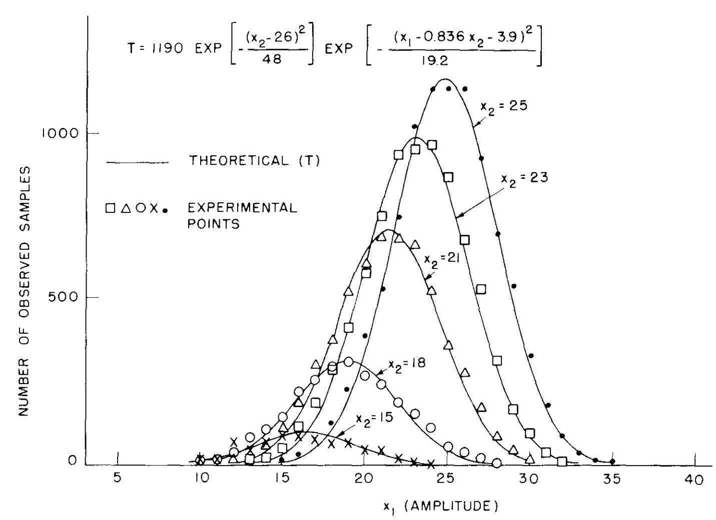

Fig. XI-4. Second-order probability density of Gaussian noise.

In the measurement of this density, one random variable, say x_2, is held at a certain value while a slice of the surface is taken for this value. This creates a family of curves plotted against x_1, with x_2 as a parameter. A form of Eq. 1 that is more useful for this representation is

$$p(x_1, x_2) = \frac{1}{2\pi\, \sigma_1 \sigma_2 (1-\rho^2)^{1/2}} \exp\left[-\frac{(x_2-m_2)^2}{2\sigma_2^2}\right] \exp\left[-\frac{\left(x_1 - m_1 - \frac{\sigma_1\rho}{\sigma_2} x_2 + \frac{\sigma_1\rho}{\sigma_2} m_2\right)^2}{2\sigma_1^2(1-\rho^2)}\right]$$

The individual curves of the family have the maximum values

$$\left[p_{x_2}(x_1)\right]_{max} = \frac{1}{2\pi\, \sigma_1\sigma_2(1-\rho^2)^{1/2}} \exp\left[-\frac{(x_2-m_2)^2}{2\sigma_2^2}\right] \tag{2}$$

at

$$x_1 = \frac{\sigma_1\rho}{\sigma_2} x_2 + m_1 - \frac{\sigma_1\rho}{\sigma_2} m_2 \tag{3}$$

and variance, $\sigma_1^2(1-\rho^2)$. The positions of the maxima lie on a straight line on the x_2, x_1 plane with slope $\sigma_2/\sigma_1\rho$. The plot of the experimental maxima of the data shown in Fig. XI-4 is given in Fig. XI-5. All the pertinent parameters can be obtained in a manner similar to that described for the first-order case from the plots of Eqs. 2 and 3, and from the individual curves of Fig. XI-4.

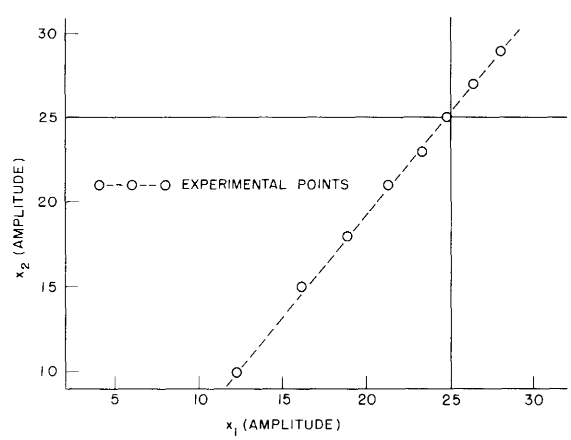

Fig. XI-5. Plot of maxima of slices.

1. The Measurement System

The system of measurement used here consists, ideally, of creating a movable "window" or "aperture" within the amplitude range of the process. The process is then sampled a finite number of times, and those samples that appear within the aperture are counted. The ratio of the number counted to the total number taken is an approximation to the probability density at the center of the aperture.

2. Error Analysis

Before any form of "goodness-of-fit" test can be applied, an investigation of errors introduced by the measurement must be made. There are two kinds of error involved here, those caused by aperture width (a form of quantization error) and those caused by finite sample size. The first is a consistent error, the second is statistical.

The effect of aperture width on the measurement of a probability density p(x) is the approximation of the value of p(x) at the center of the aperture by the integral of p(x) over the aperture, divided by the aperture width; that is,

$$p(x_i) \approx \frac{1}{\epsilon} \int_{x_i-\epsilon/2}^{x_i+\epsilon/2} p(x)\, dx = \frac{P_i}{\epsilon} \tag{4}$$

where P_i is the probability of the event $[x_i - \epsilon/2 \leq x < x_i + \epsilon/2]$, and ϵ is the aperture width. Applying Taylor's theorem to p(x), we have

$$p(x) = p(x_i) + \frac{P'(x_i)}{1!} (x - x_i) + \frac{P''(x_i)}{2!} (x - x_i)^2 + R(x) \tag{5}$$

where

$$R(x) = \frac{p'''(\xi)}{3!} (x - x_i)^3$$

and ξ lies between x and x_i. Applying the integral (Eq. 4), we obtain

$$\frac{1}{\epsilon} \int_{x_i-\epsilon/2}^{x_i+\epsilon/2} p(x)\, dx = p(x_i) + p''(x_i) \frac{\epsilon^2}{24} + \Psi(x_i) \tag{6}$$

Thus the quantization error can be expressed as

$$e(x_i) = p''(x_i) \frac{\epsilon^2}{24} + \Psi(x_i) \tag{7}$$

where $\Psi(x_i)$ is a remainder term. A bound on $|\Psi(x_i)|$ can be found.

$$|\Psi(x_i)| = \left| \frac{1}{\epsilon} \int_{x_i-\epsilon/2}^{x_i+\epsilon/2} R(x)\, dx \right| \leqslant \frac{1}{\epsilon} \int_{x_i-\epsilon/2}^{x_i+\epsilon/2} |R(x)|\, dx$$

$$\leqslant \frac{\theta(x_i)}{\epsilon\, 3!} \int_{x_i-\epsilon/2}^{x_i+\epsilon/2} |x - x_i|^3\, dx = \frac{\theta(x_i)}{192}\, \epsilon^3$$

therefore

$$|\Psi(x_i)| \leqslant \theta(x_i) \frac{\epsilon^3}{192}$$

where $|p'''(x)| \leqslant \theta(x_i)$, $x_i - \epsilon/2 \leqslant x < x_i + \epsilon/2$; that is, $\theta(x_i)$ is an upper bound for $|p'''(x)|$ within the aperture.

The effects of a finite sample size can be found by application of certain results in sampling theory (7). Here the sampled function is considered, in effect, as a function $\phi_i(t)$, defined as follows.

$$\phi_i(t) = \begin{cases} 1 & x_i - \frac{\epsilon}{2} \leqslant x(t) < x_i + \frac{\epsilon}{2} \\ 0 & \text{elsewhere} \end{cases}$$

The samples of $\phi_i(t)$ are

$$\phi_i^{(1)}, \phi_i^{(2)}, \ldots, \phi_i^{(j)}, \ldots, \phi_i^{(N)}$$

where $\phi_i^{(j)} = \phi_i(t_j)$, and N is the total number of samples. The $\phi_i^{(j)}$ are random variables, each of which has a probability distribution

$$P\left[\phi_i^{(j)} = 1\right] = P_i$$

$$P\left[\phi_i^{(j)} = 0\right] = 1 - P_i$$

The sample mean,

$$M_i = \frac{1}{N} \sum_{j=1}^{N} \phi_i^{(j)}$$

is the frequency ratio of the event $[x_i - \epsilon/2 \leq x(t_j) < x_i + \epsilon/2]$, and it can be shown that its variance is

$$\sigma^2[M_i] = \frac{P_i(1 - P_i)}{N} \tag{8}$$

A reasonable measure of this error is $2\sigma[m_i]$, since the error, if Gaussian, is less than this 95 per cent of the time.

Errors were computed for the measurement of Fig. XI-3 at the point $x = 0$, where both kinds of error are maximum. For $\epsilon = 1$, the estimate of total error, from Eqs. 7 and 8,

$$E_t = 2\sigma[M_i] + e(x_i)$$

was found to be 4.2 per cent of $p(0)$; for $\epsilon = 2$, 3.3 per cent; and for $\epsilon = 4$, 4.3 per cent. An aperture width of two was chosen for the measurement. An estimate of 7 per cent was computed for the measurement of Fig. XI-4. The points are seen to lie well within this measure of error; the error estimates are pessimistic, however, since they were computed for the worst possible case.

Increasing the aperture width decreases the statistical error and increases the quantization error. If interest lies only in measurement of the moments of the distribution, the aperture width may be increased even more than we have indicated, and thereby the statistical irregularity may be reduced. The quantization error may then be reduced under certain conditions by application of Sheppard's corrections (8). If the characteristic function satisfies certain restrictions, the original $p(x)$ can be retrieved from the experimental points P_i by methods similar to those of the sampling theorem (9). Iterative procedures with the use of the formula,

$$P_i = p(x_i) + p''(x_i)\,\frac{\epsilon^2}{24} + p''''(x_i)\,\frac{\epsilon^4}{1920} + \dots$$

should also be successful in some cases.

K. L. Jordan, Jr.

References

1. H. E. Singleton, A digital electronic correlator, Technical Report 152, Research Laboratory of Electronics, M.I.T., Feb. 21, 1950; Proc. IRE 38, 1422 (1950).
2. Quarterly Progress Report, Research Laboratory of Electronics, M.I.T., April 15, 1956, pp. 69-70.
3. K. L. Jordan, Jr., A digital probability density analyzer, S.M. Thesis, Department of Electrical Engineering, M.I.T., Sept. 1956.

4. J. D. Cobine, Noise output of the Sylvania 6D4 gas triode at audio and supersonic frequencies, NDRC Report 411-92, May 29, 1944.

5. H. Cramér, Mathematical Methods of Statistics (Princeton University Press, Princeton, N.J., 1946), pp. 323-325, 416-452.

6. W. B. Davenport and W. L. Root, Random Signals and Noise (McGraw-Hill Publishing Company, New York, 1958), p. 149.

7. Ibid., pp. 76-79.

8. H. Cramér, op. cit., pp. 359-363.

9. B. Widrow, A study of rough amplitude quantization by means of Nyquist sampling theory, Sc.D. Thesis, M.I.T., 1956, pp. 17-22.